論文の内容の要旨

論文題目：

Synthesis and Characterization of Vertically Aligned Single-Walled Carbon Nanotubes

（垂直配向単層カーボンナノチューブ膜の合成と評価）

エイナルソン　エリック

1. Introduction

The role of single-walled carbon nanotubes (SWNTs) is becoming increasingly important, with synthesis and analysis techniques advancing at a very quick pace. In just the past few years, synthesis of high-purity, vertically aligned (VA-)SWNTs has been realized [1-3], adding a great boost to the field of nanotechnology. In addition, characterization methods have also matured, allowing one to better characterize the SWNTs being produced. However, there are still many areas that are not yet well understood, such as the details of the SWNT growth process and how to accurately control the morphology of SWNTs.

In this study, the growth mechanism of vertically aligned SWNTs was investigated using a newly developed optical technique [4,5] that allows real-time observation of the growth. This study helped to clarify the growth process, which was described by an analytical growth model. The morphology of the vertically aligned SWNT films was also investigated using several spectroscopic techniques.

2. Synthesis of vertically aligned SWNTs from alcohol

The VA-SWNTs used in this study were grown on quartz substrates by the alcohol catalytic CVD process [6]. An FE-SEM image of VA-SWNTs produced by the alcohol CVD method is shown in Fig. 1a. In the corresponding resonance Raman spectrum (Fig. 1b), the presence of a strong, sharp peak at 1593 cm^{-1} (the G-band) and radial breathing

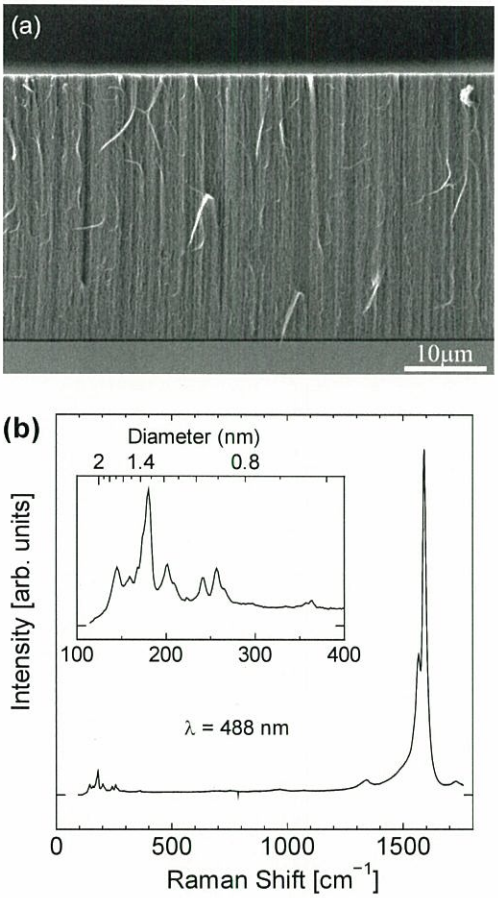

Fig. 1 (a) Vertically aligned SWNTs synthesized from alcohol. The film thickness exceeds 30 μm. (b) A typical Raman spectrum from the VA-SWNTs (RBM shown in detail in the insert).

mode (RBM) peaks between 100 and 400 cm^{-1} reveal the presence of SWNTs [7]. The weak intensity of the D-band peak near 1340 cm^{-1} relative to the G-band indicates the pristine sample is of high purity. In the RBM region, a dominant peak at 180 cm^{-1} indicates the SWNTs in the sample are vertically aligned [8].

In situ optical absorbance measurements of the VA-SWNT film growth were performed as follows. An optically polished quartz substrate, on which Co/Mo catalyst had been supported by a dip-coat catalyst loading method [9], was positioned in the CVD furnace such that a laser (λ = 488 nm) was incident normal to the substrate through a small opening in the bottom of the furnace. The transmitted light passed through another small opening in the top of the furnace, where the intensity was measured. Beer's Law was used to determine the absorbance from the relative transmitted intensity. Based on the correlation between the thickness of the VA-SWNT film and its absorbance [4], the film growth could be directly measured using this method.

2.1 Formulation of the growth model

It is believed the VA-SWNTs grow from catalyst particles that remain on the surface during growth. The flux of carbon feedstock (alcohol vapor) supplied to the catalyst at the substrate surface, is J [mol μm^{-2} s^{-1}]. The catalyst activity was defined as the proportion of available carbon (J) to the amount (in moles) of SWNTs produced by the reaction. Hence, the molar growth rate of the VA-SWNT film, $\eta(t)$ [mol μm^{-2} s^{-1}], has units of flux.

Data obtained by *in situ* absorbance measurements (Fig. 2a) show the progression of VA-SWNT film growth with CVD reaction time. The growth rate is clearly fastest at the onset of growth, and decreases in an exponential fashion as CVD time progresses, indicating the slowing growth rate is due to diminishing catalyst activity rather than a diffusion-limited mechanism. This decrease in catalyst activity may be due to byproducts from alcohol decomposition reacting with the catalyst particles before diffusing away from the substrate surface, or to the formation of amorphous carbon around the catalyst particles. Both of these processes are driven by the alcohol decomposition reaction, thus it is postulated that the rate at which the catalyst activity diminishes is proportional to the rate of alcohol dissociation [10] by some constant κ [s^{-1}], as expressed by

$$-\frac{d\eta(t)}{dt} = \kappa\eta(t) \tag{1}$$

Solving (1) yields the time-dependent molar growth rate,

$$\eta(t) = \eta_0 e^{-t/\tau} \tag{2}$$

where η_0, is the initial molar growth rate (at t = 0), and τ [s], defined by $\tau \equiv \kappa^{-1}$, is the effective catalyst lifetime. Assuming the molar density ρ_{mol} of the VA-SWNT film is uniform over the area of the laser spot, we can define the growth rate by $\gamma(t) = \eta(t)/\rho_{mol}$ where $\gamma_0 = \gamma(t=0)$ is the initial growth rate. The VA-SWNT film growth rate $\gamma(t)$ [μm s^{-1}] can then be expressed by an equation of the same form as (2),

$$\gamma(t) = \gamma_0 e^{-t/\tau} \tag{3}$$

The film thickness $H(t)$ [μm] is thus

$$H(t) = \int \gamma(t) dt \tag{4}$$

Given that $H(t=0) = 0$, the film thickness is

$$H(t) = \gamma_0 \tau \left(1 - e^{-t/\tau}\right) \tag{5}$$

Data obtained from *in situ* optical absorbance measurements can be fit using equation (5). Three different cases are shown in Fig. 2a,

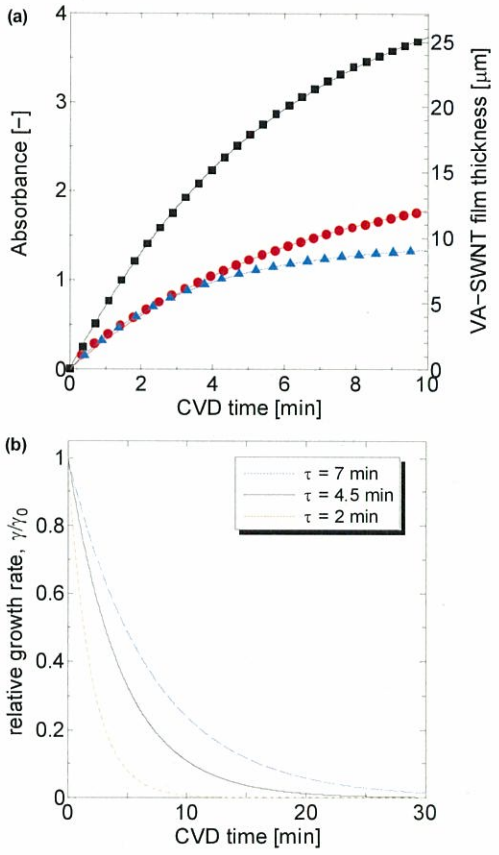

Fig. 2 (a) Growth data obtained for different VA-SWNT films by *in situ* optical absorbance measurements, and fitted curves calculated using eqn. (5). (b) Exponential decay of the catalyst activity with reaction time. The solid line corresponds to the average τ determined from fitting. Dashed lines represent upper/lower bounds.

where the solid curves were fit to measured absorbance data (indicated by the markers). The initial growth rate γ_0 and catalyst time constant τ were determined simultaneously by iterative fitting. The average value obtained from several cases was $\tau = 4.5$ minutes. Based on this value, the decay of the growth rate is plotted in Fig. 2b. The solid black line was calculated using equation (2), and the dashed lines show the standard deviation. According to this plot, γ typically diminishes to less than 5% of γ_0 in approximately 15 min, thus no significant growth occurs for longer CVD times.

The excellent fit (R^2 values ≥ 0.99) shows that the above model accurately describes VA-SWNT film growth. It is interesting to note that equation (5) has the same form as that reported by Futaba *et al.* [11], despite very different experimental conditions. The catalyst lifetime is also nearly the same (~4.5 min), although see no decrease in the catalyst lifetime for higher initial growth rates, which supports our initial assumption that both are driven by the same reaction.

3. Determining the internal structure of the VA-SWNT film

We investigated the internal structure of freestanding VA-SWNT films using electron scattering, electron energy-loss spectroscopy (EELS), and transmission electron microscope (TEM) observation. These studies reveal the films are comprised of very small SWNT bundles and individual SWNTs. This is a significant find because many of the potential applications of SWNTs that have been

proposed since their discovery [12] are based on exploiting the novel physical properties arising from their one-dimensionality [13]. However, this 1D nature is often lost to bundling of SWNTs during production. In particular, the effects of bundling on the electronic structure of SWNTs have been addressed in many reports in the literature [14-18]. Significant bundling not only dashes the hopes of many proposed applications, but makes measurements of some fundamental physical properties of SWNTs all the more challenging.

3.2 X-Ray Absorbance (XAS)

XAS was performed on VA-SWNTs using highly polarized synchrotron radiation. Absorption of X-rays usually occurs by excitation of core electrons into the conduction band. The carbon atoms in SWNTs are sp^2 hybridized [13], thus excitation into the π (σ) bands can occur. Since these bands are oriented perpendicular (parallel) to the SWNT axis, the degree of alignment of the SWNTs can be determined from an analysis of the anisotropy in absorbance spectra. XAS spectra obtained for a fixed incidence angle (60°) and changing polarization is shown in Fig. 3a. Anisotropy of the π core edge is clearly observed. The ratio of this peak to the σ peak is shown in Fig. 3b, and corresponds to a degree of alignment of approx. 27°. This value matches our previously obtained value of 24° obtained from polarized optical absorbance [19]. This value is also in agreement with electron scattering measurements performed on the same VA-SWNT films (not shown).

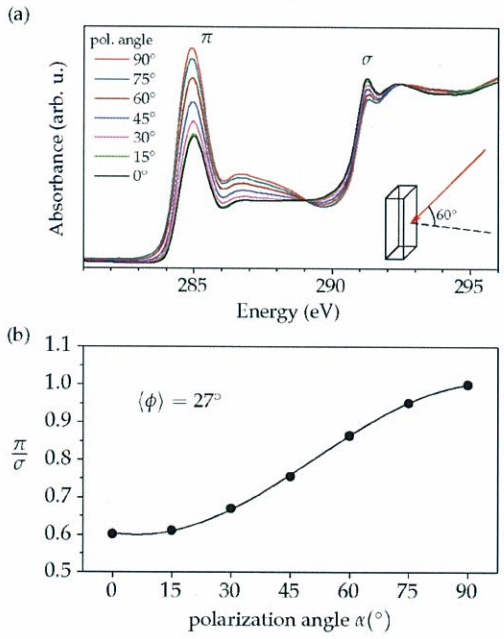

Fig. 3 (a) X-ray absorbance spectra showing strong anisotropy of the core edge, due to alignment of the SWNTs. (b) The π to σ peak ratio vs. polarization angle, which indicates the SWNTs are aligned within ≈27° of the substrate normal

3.2 TEM observation

VA-SWNT films were removed from the quartz substrate on which they were grown, and transferred onto TEM grids using a simple hot-water assisted process [20]. This process conserves SWNT alignment, resulting in a freestanding VA-SWNT film sitting atop a TEM grid. The VA-SWNTs were then observed from the top of the film, looking along the alignment direction. The sparse, relatively homogeneous film structure is shown in Fig. 4a. The dark spots dotting the image are not metal particles or carbonaceous impurities, but are cross-sections of SWNT bundles. Due to the alignment of the film, a large number of bundle

cross-sections are observed. Figure 4b shows the size of the bundles, which typically contain only 3-10 SWNTs. Individual nanotubes are also found dispersed throughout the film. Images in Fig. 4a and 4b are from a 2 μm thick VA-SWNT film at an operating voltage of 300 kV. Figure 4c is from a 7 μm-thick film, and was taken at 200 kV. The observed internal structure is basically the same for both films. Based on these images, we find the internal structure of aligned SWNT films is not as well ordered as one might deduced from SEM observation. Furthermore, the bundles comprising the films are unexpectedly small, which is expected to significantly affect the electronic properties of the VA-SWNT films.

3.3 Electron Energy-Loss Spectroscopy (EELS)

High-resolution EELS measurements were performed at room temperature under ultra-high vacuum using a purpose-built high-resolution spectrometer having good

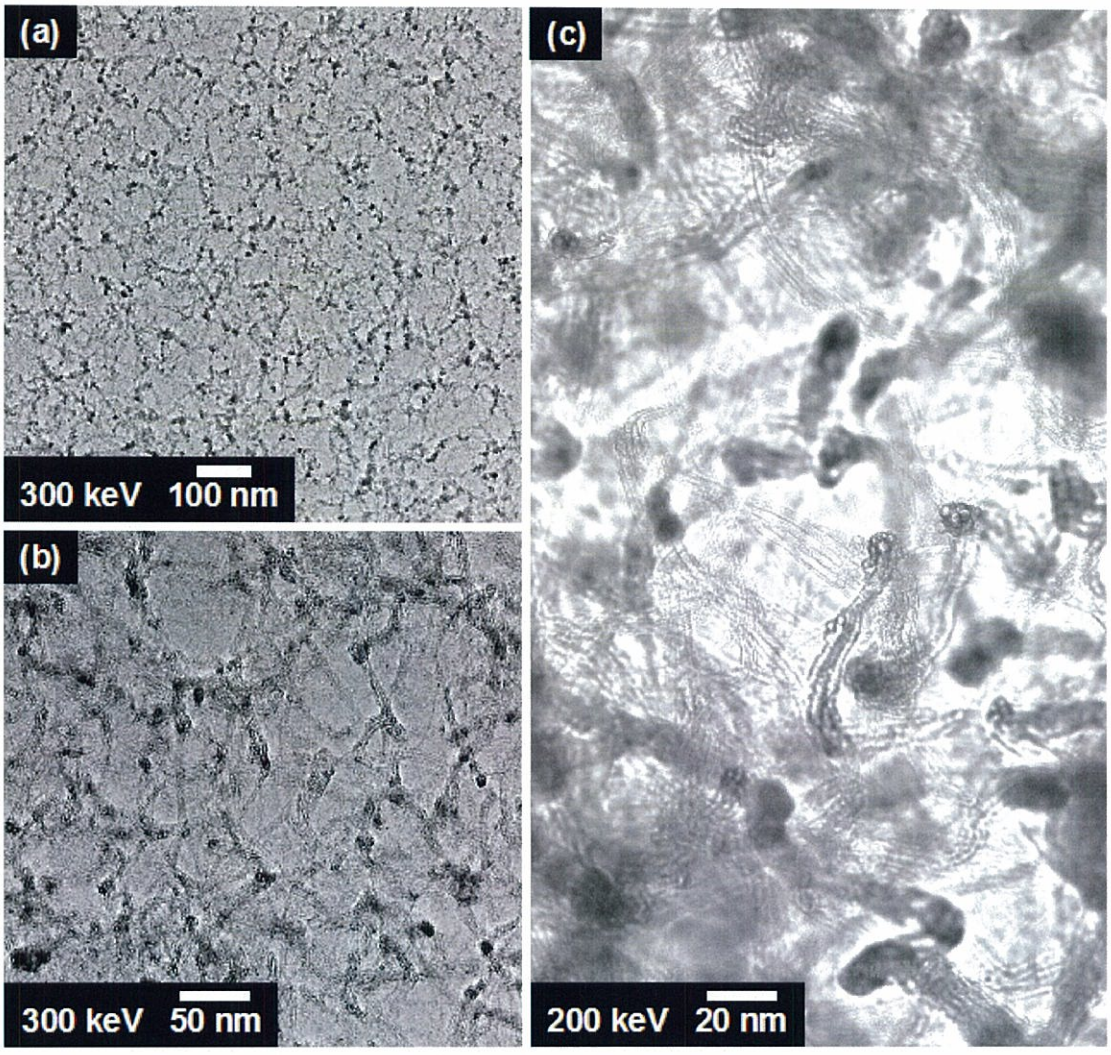

Fig. 4 TEM images looking along the alignment direction of a freestanding VA-SWNT film. The many dark spots in (a) are cross-sections of small SWNT bundles, shown in (b) and (c). Images (a) and (b) were taken at 300 keV with a Tecnai F30, while (c) was taken at 200 kV with a JEM-2000EX microscope

energy and momentum resolution [21]. The energy of the π-plasmon (arising from a collective excitation in the π electrons [22]) is shown in Fig. 5a for various degrees of momentum transfer, q (0.1 to 0.8 $Å^{-1}$). The filled squares correspond to this study, while the open circles are data from a previous study on magnetically aligned SWNT bundles [23]. In both cases there is a clear momentum-dependent dispersion, but the dispersion is much larger in the VA-SWNTs (squares) than in the magnetically aligned SWNT bundles (circles). This is attributed to the small bundle size observed by TEM (containing 3 to 10 SWNTs). In such a bundle, only one or two of the SWNTs will be surrounded by other SWNTs (i.e. in the "bulk" of the bundle). As a result, almost all of the nanotubes are on the bundle surface, thus one expects insignificant changes in the dielectric response function of the SWNTs. Early

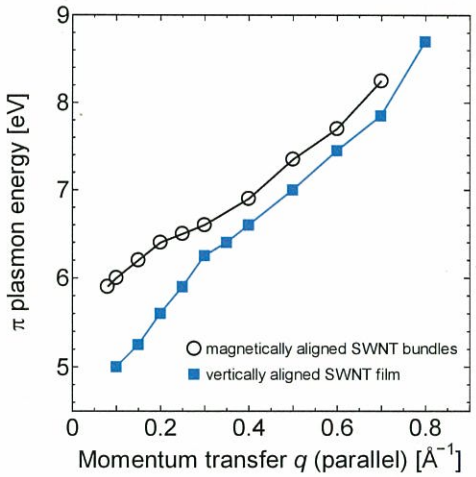

Fig. 5 Momentum-dependent dispersion of the π plasmon energy for VA-SWNTs (filled squares) is much larger than for magnetically aligned SWNT bundles (open circles), indicating minimal tube-tube shielding effects.

calculations by Lin *et al.* [24] show the dispersion of the π plasmon in individual SWNTs should be larger than in bundles, in agreement with our findings. These results indicate the SWNTs in the vertically aligned film are sufficiently unbundled to retain the 1D electrical nature of the component SWNTs.

By setting the momentum transfer to zero in the EELS spectrometer, one can perform electron diffraction (ED) measurements. In the ED measurements on the VA-SWNTs investigated here (not shown), no bundle peak was observed in the low momentum-transfer region (below 2 $Å^{-1}$). This adds further support to the TEM and EELS results showing the degree of bundling of SWNTs in these aligned films is rather insignificant. The SWNT orientation is also in agreement with the value found by XAS and optical absorbance measurements.

4. Conclusion

In summary, we have investigated the growth process of VA-SWNT films, and have developed an analytical model to explain the process. The degree of alignment of the SWNTs determined from X-ray absorbance spectra was approximately 27°, in agreement with the 24° obtained from polarized optical absorbance. TEM observations along the alignment direction of the VA-SWNT films have been performed for the first time. These observations reveal the SWNTs within the film form unexpectedly small bundles (containing 3 to 10 SWNTs). The lack of bundling observed by TEM observations is supported by EELS

measurements on the aligned SWNT films, which indicate the overall electronic properties of the film are dominated by individual SWNTs rather than bulk SWNT bundles. These findings are very interesting and promising for future studies on the 1D properties of SWNTs.

REFERENCES

[1] Y. Murakami, S. Chiashi, Y. Miyauchi, M. Hu, M. Ogura, T. Okubo, S. Maruyama, *Chem. Phys. Lett.* **385** (2004) 298.

[2] K. Hata, D.N. Futaba, K. Mizuno, T. Namai, M. Yumura, S. Iijima, *Science* **306** (2004) 1362.

[3] G. Zhong, T. Iwasaki, K. Honda, Y. Furukawa, I. Ohdomari, H. Kawarada, *Chem. Vap. Dep.* **11** (2005) 127.

[4] S. Maruyama, E. Einarsson, Y. Murakami, T. Edamura, *Chem. Phys. Lett.* **403** (2006) 320.

[5] E. Einarsson, M. Kadowaki, Y. Murakami, S. Maruyama, *in preparation.*

[6] S. Maruyama, R. Kojima, Y. Miyauchi, S. Chiashi, M. Kohno, *Chem. Phys. Lett.* **360** (2002) 229.

[7] M.S. Dresselhaus & P. Eklund, "Phonons in Carbon Nanotubes", *Adv. in Phys.* **49** (2000) 705.

[8] Y. Murakami, S. Chiashi, E. Einarsson, S. Maruyama, *Phys. Rev. B* **71** (2005) 085403.

[9] Y. Murakami, Y. Miyauchi, S. Chiashi, S. Maruyama, *Chem. Phys. Lett.* **377** (2003) 49.

[10] Y. Murakami, PhD Thesis, "CVD Growth of Single-Walled Carbon Nanotubes and their Anisotropic Optical Properties", The University of Tokyo, 2005.

[11] D.N. Futaba, K. Hata, T. Yamada, K. Mizuno, M. Yumura, S. Iijima, *Phys. Rev. Lett.* **95** (2005) 056104.

[12] S. Iijima & T. Ichihashi, *Nature* **363** (1993) 603.

[13] R. Saito, G. Dresselhaus, M.S. Dresselhaus, "Physical Properties of Carbon Nanotubes" Imperial College Press, London, 1998.

[14] P. Delaney, H.J. Choi, J. Ihm, S.G. Louie, M.L. Cohen, *Nature* **391** (1998) 466.

[15] Y.K. Kwon, S. Saito, D. Tománek, *Phys. Rev. B* **58** (1998) R13314.

[16] A.A. Maarouf, C.L. Kane, E.J. Mele, *Phys. Rev. B* **61** (2000) 11156.

[17] M. Ouyang, J.-L. Huang, C.L. Cheung, C.M. Leiber, *Science* **292** (2001) 702.

[18] S. Reich, C. Thomsen, P. Ordejón, *Phys. Rev. B* **65** (2002) 155411.

[19] Y. Murakami, E. Einarsson, T. Edamura, S. Maruyama, *Phys. Rev. Lett.* **94** (2005) 087402.

[20] Y. Murakami & S. Maruyama, *Chem. Phys. Lett.* **422** (2006) 575.

[21] J. Fink, *Adv. Electron. Electron Phys.* **75** (1989) 121.

[22] T. Pichler, M. Knupfer, M.S. Golden, J. Fink, A. Rinzler, R.E. Smalley, *Phys. Rev. Lett.* **80** (1998) 4729.

[23] X. Liu, T. Pichler, M. Knupfer, M.S. Golden, J. Fink, D.A. Walters, M.J. Casavant, J. Schmidt, R.E. Smalley, *Phys. Rev. B* **66** (2002) 045411.

[24] M.F. Lin & D.S. Chuu, *Phys. Rev. B* **57** (1998) 10183.